Communication

A Polar Oxide with a Large Magnetization Synthesized at Ambient Pressure

Helen Hughes, Mathieu M. B. Allix, Craig A. Bridges, John B. Claridge, Xiaojun Kuang, Hongjun Niu, Stephen Taylor, Wenhai Song, and Matthew J. Rosseinsky

J. Am. Chem. Soc., **2005**, 127 (40), 13790-13791• DOI: 10.1021/ja054839w • Publication Date (Web): 20 September 2005

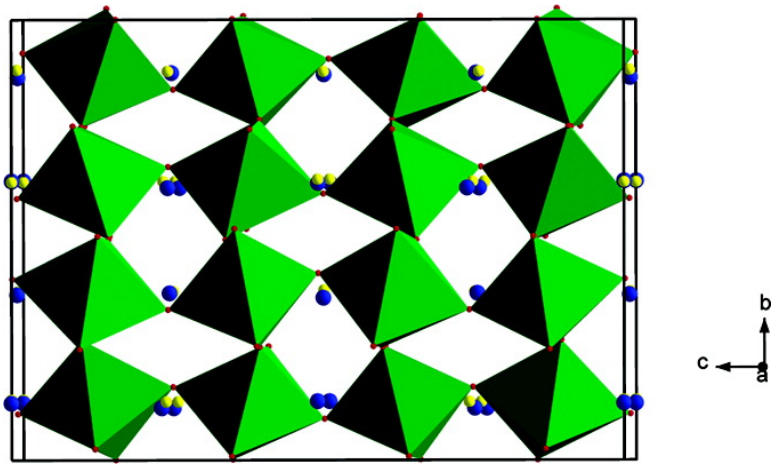

More About This Article

Additional resources and features associated with this article are available within the HTML version:

- Supporting Information
- Links to the 11 articles that cite this article, as of the time of this article download
- Access to high resolution figures
- Links to articles and content related to this article
- Copyright permission to reproduce figures and/or text from this article

View the Full Text HTML

J|A|C|S
COMMUNICATIONS

Published on Web 09/20/2005

A Polar Oxide with a Large Magnetization Synthesized at Ambient Pressure

Helen Hughes,[†] Mathieu M. B. Allix,[†] Craig A. Bridges,[†] John B. Claridge,[†] Xiaojun Kuang,[†] Hongjun Niu,[†] Stephen Taylor,[‡] Wenhai Song,[‡] and Matthew J. Rosseinsky*[,†]

Department of Chemistry, University of Liverpool, Liverpool L69 7ZD, U.K., and Department of Electrical Engineering and Electronics, University of Liverpool, Liverpool, L69 3GJ U.K.

Received July 19, 2005; E-mail: m.j.rosseinsky@liv.ac.uk

Multifunctional systems are an important current focus in materials research due to the fundamental and technological opportunities arising from coupling of distinct order parameters. For example, ferromagnetic ferroelectrics[1] permit magnetic control of electrical polarization and associated multiple state memory applications. The design of materials with both ferroelectric polarization and ferromagnetic magnetization is complicated by the conflicting electronic requirements of these properties: ferromagnetism requires the presence of d-electrons, whereas ferroelectricity in $BaTiO_3$ arises from structural displacements driven by bonding characteristic of the d^0 Ti(IV) center. One strategy to overcome this is to decouple the metal centers responsible for ferroelectricity and ferromagnetism by using separate ions to produce the required ordering. Ferromagnetism and ferroelectricity coexist in $BiMnO_3$[2], an Mn^{3+} phase accessible only under high pressure: orbital ordering at Mn^{3+} produces the ferromagnetism, whereas the lone pair at Bi^{3+} drives the ferroelectric distortion.[3,4]

Multiple cation occupation of the octahedral B site in the ABO_3 perovskite structure can generate ferromagnetism by exploiting the ferromagnetic σ superexchange interaction between e_g^n ($n = 1, 2$) and e_g^0 cations. Polarity can then be embedded within the ferromagnetic BO_3 network using a stereochemically active A cation. Starting with a target of Mn^{4+} and Ni^{2+} as the ferromagnetically coupled cations on the B site[5] and Bi^{3+} as the A-site cation, we have prepared a polar spin-glass oxide with a large low-temperature magnetization. This material can be prepared at ambient pressure and grown as single crystals. This is chemically remarkable as neither $BiMnO_3$ nor $BiNiO_3$[6] can be synthesized at ambient pressure and opens up the synthesis of multiple B-site multiproperty perovskites at ambient pressure.

The initial target was the composition Bi_2MnNiO_6 (reported by high-pressure synthesis by Azuma et al. during the course of this work[7]). Reaction of Bi_2O_3, MnO_2, and NiO in air at ambient pressure under a range of reaction conditions afforded a multiphase product which however did contain a perovskite-like phase. Investigation of the elemental composition of the components of this multiphase assemblage using EDX on approximately 50 crystallites revealed that this perovskite phase had metal ratios corresponding to the composition $Bi_2Mn_{4/3}Ni_{2/3}O_x$. Synthesis at this composition under conditions designed to minimize Bi loss afforded a perovskite-related material with minimal impurity (NiO, $Bi_{12}MnO_{20}$) contamination. Redox titration of the oxygen content gave the overall composition $Bi_2Mn_{4/3}Ni_{2/3}O_6$. This corresponds to B-site occupancy by 33% Mn^{4+}, 33% Mn^{3+}, and 33% Ni^{2+}, i.e., a reduced Mn oxidation state in comparison with the high-pressure Mn^{4+} phase Bi_2MnNiO_6.[7] The reciprocal space was reconstructed for characteristic crystallites from electron diffraction patterns by tilting around the crystallographic axes, revealing an orthorhombic perovskite-related cell with $a \approx \sqrt{2}a_p$, $b \approx 2\sqrt{2}a_p$, and $c \approx 4a_p$ (a_p is the parameter of the cubic perovskite subcell). No condition limiting the general *hkl* reflections was observed, suggesting a *P* lattice. The only extra condition, $0kl$: $k + l = 2n$ due to an *n* glide along *a*, restricts the choice to one of the space groups *Pnmm*, $Pn2_1m$, and $Pnm2_1$ (Figure 1).

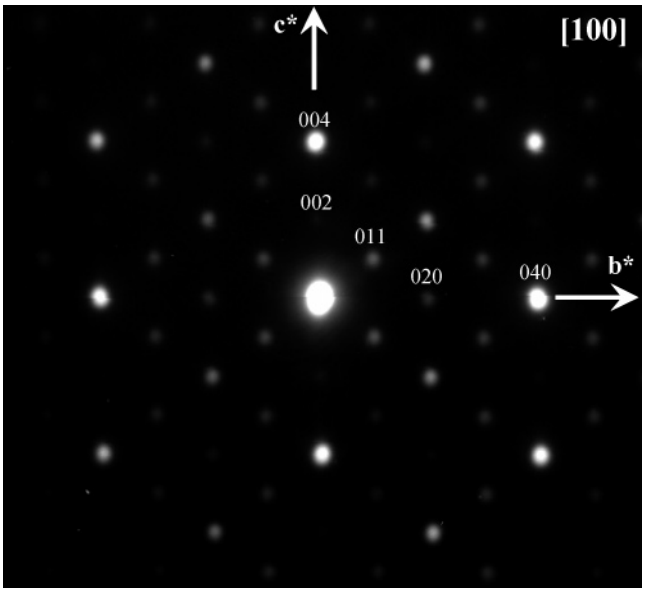

Figure 1. [100] electron diffraction pattern of $Bi_2Mn_{4/3}Ni_{2/3}O_6$.

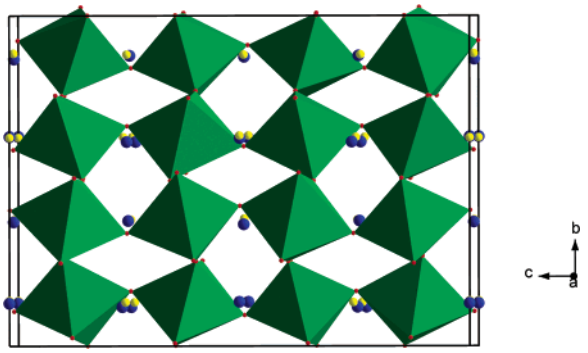

Figure 2. Polar displacements of the Bi cations (blue) along the *b* axis away from the centroids of their O coordination environments (yellow) in $Bi_2Mn_{4/3}Ni_{2/3}O_6$.

The structure (Figure 2) was solved by synchrotron single-crystal X-ray diffraction data collected on a 20 μm fragment cut from a flux-grown single crystal, which confirms the space group as $Pn2_1m$; no satisfactory refinement could be obtained in nonpolar *Pnmm*. Synchrotron powder data reveal the structure to be slightly incommensurate due to a two-dimensional modulation with refined modulation vectors of $\mathbf{q}_1 = (0, -0.4967(1), 0)$ and $\mathbf{q}_2 = (0.4927(1),$

[†] Department of Chemistry
[‡] Department of Electrical Engineering and Electronics.

10.1021/ja054839w CCC: $30.25

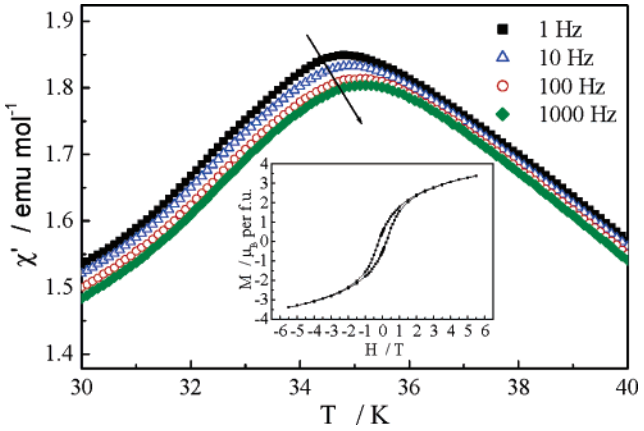

Figure 3. Frequency dependence of the ac susceptibility of $Bi_2Mn_{4/3}Ni_{2/3}O_6$ shows that the transition at 35 K is spin glass-like freezing. The inset shows the field dependence of the dc magnetization at 2 K.

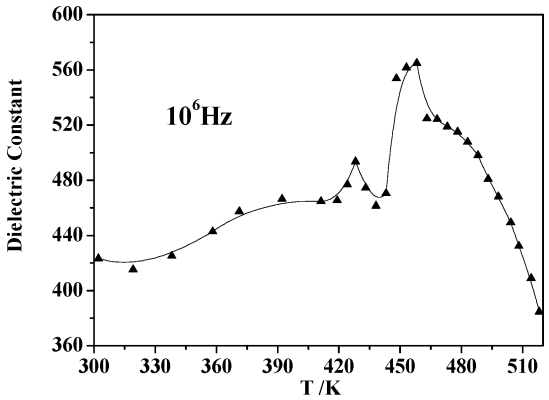

Figure 4. Relative permittivity of $Bi_2Mn_{4/3}Ni_{2/3}O_6$ measured at 10^6 Hz. The sample becomes too conducting for reliable measurement of the relative permittivity above 240 °C.

0, 0) and described by the superspace group *Ibmm*(0−*q*0,*p*00)*mm*0,[8] $a = 5.57450(6)$ Å, $b = 7.7758(1)$ Å, $c = 5.50825(8)$ Å. The polarization arises from lone-pair-driven cooperative displacements of the Bi atoms away from the centroids of their oxygen coordination polyhedra along the *b* axis, producing a calculated polarization of 60 μC cm^{-2}.

The structure analysis was confirmed by constrained refinement of neutron powder diffraction data (Figure S1), which revealed an essentially random Mn/Ni distribution over the four symmetry-independent octahedral sites. The substitutional disorder between Mn and Ni on the magnetically active B site has a decisive effect on the physical properties. The ac susceptibility has a frequency-dependent maximum in χ' (Figure 3) below 35 K, while the 2 K field-cooled dc magnetization isotherm revealed a displaced hysteresis loop with a magnetization of 3.38 μ_B per $Bi_2Mn_{4/3}Ni_{2/3}O_6$ formula unit at 5.5 T. Neutron powder diffraction at 2 K reveals no magnetic Bragg scattering. These data are consistent with the material behaving as a large magnetization concentrated spin glass below 35 K with an important role played by locally ferromagnetic Mn^{4+}/Ni^{2+} interactions. The absence of ferromagnetic long-range order can be associated with the influence of the extensive B-site disorder and the resulting antiferromagnetic Ni^{2+}/Ni^{2+} $e_g^2-e_g^2$ and Mn^{4+}/Mn^{4+} $t_{2g}^3-t_{2g}^3$ superexchange couplings.

The ac impedance spectra reveal a broad, structured peak in the real part of the dielectric permittivity, ϵ' at 10^4-10^6 Hz in the 150−240 °C temperature range (Figure 4), consistent with a ferroelectric-like transition from the polar room-temperature structure to a nonpolar high-temperature structure, confirmed by temperature-dependent X-ray powder diffraction data, which reveal a $\sqrt{2}a_p$, $\sqrt{2}a_p$, $2a_p$ cell at higher temperature. The broad nature of the permittivity maximum may also be assigned to relaxor behavior. Dielectric loss as a function of frequency (Figure S2) is also consistent with ferroelectricity. $Bi_2Mn_{4/3}Ni_{2/3}O_6$ can be prepared without the need for high-pressure synthesis despite the instability of the end-members $BiMnO_3$ and $BiNiO_3$ under ambient-pressure synthetic conditions. This may be ascribed to the optimization of the oxidation state of each octahedral cation in a multiple B-site material within the polar BiO_3 network via interplay between the accessible redox states of the selected transition metals. The mean 3+ charge on the B site can be accommodated without the need for Ni to adopt the +3 oxidation state, and the associated increase of the average Mn oxidation state to +3.5 through the formation of Ni^{2+} reduces the distorting influence of the Jahn−Teller instability of the pure Mn^{3+} state. The significance of the precise oxidation state distribution in stabilizing this composition at ambient pressure is reinforced by the observation that $Bi_2Mn_{4/3}Ni_{2/3}O_6$ is a line phase; syntheses at $Bi_2Mn_{1.4}Ni_{0.6}O_6$ and $Bi_2Mn_{1.3}Ni_{0.7}O_6$ compositions give high impurity concentrations. As site-ordered Bi_2MnNiO_6 has a Curie temperature of 140 K,[7] it is clear that enhanced function would arise from more extensive cation order on the B sites, but this may be accessible through improved design approaches, e.g., using more than two B-site cations.

Acknowledgment. We thank the UK EPSRC for Portfolio Partnership support and access to the Daresbury SRS and ISIS and ILL. MMBA acknowledges the financial support provided through the Human Potential Programme of the European Community under contract HPRN-CT-2002-00293, [SCOOTMO]. We thank P. Mallinson, A. Bowman (Liverpool), P. Henry (ILL), and M.A. Roberts (SRS) for assistance with collection of powder diffraction data and D. Bradshaw (Liverpool) and J.E. Warren (SRS) for collection of the single-crystal diffraction data.

Supporting Information Available: Synthetic procedures, experimental details for magnetization, impedance, and structural characterization (cif file). This material is available free of charge via the Internet at http://pubs.acs.org.

References

(1) Hill, N. A. *J. Phys. Chem. B* **2000**, *104*, 6694.
(2) dos Santos, A. M.; Parashar, S.; Raju, A. R.; Zhao, Y. S.; Cheetham, A. K.; Rao, C. N. R. *Solid State Commun.* **2002**, *122*, 49.
(3) Atou, T.; Chiba, H.; Ohoyama, K.; Yamaguchi, Y.; Syono, Y. *J. Solid State Chem.* **1999**, *145*, 639.
(4) Montanari, E.; Righi, L.; Calestani, G.; Migliori, A.; Giloli, E.; Bolzoni, F. *Chem. Mater.* **2005**, *17*, 1765.
(5) Dass, R. I.; Yan, J.-Q.; Goodenough, J. B. *Phys. Rev. B* **2003**, *68*, 064415.
(6) Ishiwata, S.; Azuma, M.; Takano, M.; Nishibori, E.; Takata, M.; Sakata, M.; Kato, K. *J. Mater. Chem.* **2002**, *12*, 3733.
(7) Azuma, M.; Takata, K.; Saito, T.; Ishiwata, S.; Shimakawa, Y.; Takano, M. *J. Am. Chem. Soc.* **2005**, *127*, 8889.
(8) Van Tendeloo, G.; Lebedev, O. I.; Hervieu, M.; Raveau, B. *Rep. Prog. Phys.* **2004**, *67*, 1315.

JA054839W